Author/s:
Zhang, S;Liu, M;Tan, LYF;Hong, Q;Pow, ZL;Owyong, TC;Ding, S;Wong, WWH;Hong, Y

Title:
A Maleimide-functionalized Tetraphenylethene for Measuring and Imaging Unfolded Proteins in Cells

Date:
2019-03-15

Citation:
Zhang, S., Liu, M., Tan, L. Y. F., Hong, Q., Pow, Z. L., Owyong, T. C., Ding, S., Wong, W. W. H. & Hong, Y. (2019). A Maleimide-functionalized Tetraphenylethene for Measuring and Imaging Unfolded Proteins in Cells. Chemistry an Asian Journal, 14 (6), pp.904-909. https://doi.org/10.1002/asia.201900150.

Persistent Link:
https://hdl.handle.net/11343/285427

**Title:** A Maleimide-functionalized Tetraphenylethene for Measuring and Imaging Unfolded Proteins in Cells

**Authors:** Shouxiang Zhang; Mengjie Liu; Lewis Yi Fong Tan; Quentin Hong; Ze Liang Pow; Tze Cin Owyong; Siyang Ding; Wallace Wing Ho Wong; Yuning Hong, Ph.D.



**To be cited as:** Chem. Asian J. 10.1002/asia.201900150

**Link to VoR:** https://doi.org/10.1002/asia.201900150

# A Maleimide-functionalized Tetraphenylethene for Measuring and Imaging Unfolded Proteins in Cells

Shouxiang Zhang,^[a] Mengjie Liu,^[a] Lewis Yi Fong Tan,[a] Quentin Hong,[b] Ze Liang Pow,[b] Tze Cin Owyong,[a,b] Siyang Ding,[a] Wallace W. H. Wong[b] and Yuning Hong*[a]

**Abstract:** Collapse of the protein homeostasis (proteostasis) can lead to accumulation and aggregation of unfolded proteins, which has been found to associate with a number of disease conditions including neurodegenerative diseases, diabetes and inflammation. Here we report a maleimide-functionalized tetraphenylethene (TPE)-derivatized fluorescent probe, TPE-NMI, which shows fluorescence turn-on property upon reacting with unfolded proteins in vitro and in live cells under proteostatic stress conditions. The level of unfolded proteins can be measured by flow cytometry and visualized with confocal microscopy.

## Introduction

During protein biosynthesis, the linear protein chains are subject to post-translational folding in the endoplasmic reticulum (ER) to attain their bioactive 3D conformation. This crucial activity is continuously governed by a series of quality control machinery that are collectively known as "proteostasis". In brief, proteostasis involves a complex network of molecular chaperones that assist in restoring the correct conformation of unfolded and misfolded proteins, and directing those unrepairable proteins to proteasomes for degradation.[1] In stressed and diseased cells, the excessive formation of unfolded and misfolded proteins can eventually overwhelm and impair the proteostasis machinery, causing accumulation and aggregation of the dysfunctional proteins in the ER and other intracellular compartments.[1a, 1b, 2] This phenomenon has been observed in a number of pathological conditions such as neurodegeneration, endocrine disorders, autoimmune and inflammatory diseases.[2a, 2c, 3] In this regard, research tools capable of quantifying the proteostasis capacity may provide valuable insight on the underlying causes of biological abnormalities at the cellular level, and become clinically important agents for early disease diagnosis and ongoing disease monitoring.

Convenient methods for specifically assessing the cellular proteostasis capacity are continuously being sought. To measure the level of proteostasis, the most commonly used approach to-date is by expression of metastable proteins prone to aggregation. These proteins are usually tagged with fluorescent reporters, either fluorescent proteins or chemical probes, and the extent of aggregation can be visualized and used as a proxy for proteostasis.[4] For example, Hartl and Raychaudhuri *et al.* reported the use of thermal-labile luciferase fused with fluorescent protein firefly luciferase mutants as proteostasis sensors, which luminesced in response to the changes in solubility that occurred during protein unfolding.[4a] Zhang *et al*. reported a conjugate of a chemical probe and a *de novo* designed enzyme, which formed fluorescent aggregates in the presence of cellular stress.[4b] A similar approach utilizing a fluorogenic probe targeting an aggregation-prone "HaloTag" protein mutant has also been reported.[4c, 4d] Additionally, other methods that focus on cell lysate analysis have also been documented.[4e] In general, these existing approaches are dependent on indirect indications that manifest during proteostasis imbalance. Methods that can directly report endogenous proteins that undergo unfolding in the cellular environment are still in demand.

Recently, we have reported a thiol-reactive tetraphenylethene (TPE)-derived probe, TPE-MI, for measuring unfolded proteins to reflect on proteostasis imbalance in stressed cells.[5] Cysteine (Cys) is the amino acid that is highly reactive and usually buried inside the folded protein structure. Upon protein unfolding, the buried free Cys residues became surface-exposed and accessible by the maleimide (MI) moiety, which specifically reacted with the Cys thiols via Michael addition reaction under physiological conditions.[5b, 6] Importantly, the MI moiety quenched the fluorescence of the entire molecule through photoinduced electron transfer (PeT) process. Upon reacting with thiol, the PeT effect was removed and the fluorescence was resumed.[5a] On the other hand, as a typical aggregation-induced emission (AIE) fluorogen, the TPE fluorescence was suppressed in solution when the four periphery phenyl rings underwent active intramolecular motions that deactivate the excited state species. This is particularly important in our application: the reaction with unfolded proteins where the hydrophobic patch exposed would contribute to the restriction of intramolecular motions and the enhancement of fluorescence. TPE-MI has been further applied in reporting proteostasis imbalance in Huntington's disease cell models, as well as protein damage in malaria parasites after treated with anti-malarial drugs.[5b]

TPE-MI has proved the concept of using thiol-reactive AIE fluorogens for measuring cellular unfolded proteins. However, when preparing the TPE-MI stock solution for biological testing, the concentration could not exceed 1-2 mM in DMSO owing to its strong hydrophobicity. Higher concentration of the stock solution could result in precipitation of the dye when diluting in aqueous solution. Another shortcoming of TPE-MI is that its absorption maximum falls within the ultraviolet spectral region (approx. 325 nm), which is not compatible with the commonly used 405 nm laser in most of the flow cytometers and confocal microscopy. In this work, we aimed to solve these issues by synthesizing novel structural analogs of TPE-MI that incorporates two hydrophilic groups (**Figure 1**). One of the two analogs, TPE-NMI, showed red-shift in its spectral profile and improved water solubility. Comparing with the parent compound,

[a] S. Zhang, Dr. M. Liu, L. Y. F. Tan, T. C. Owyong, S. Ding, Dr. Y.Hong
Department of Chemistry and Physics, La Trobe Institute for Molecular Science, La Trobe University, Melbourne, VIC 3086, Australia
Email: Y.Hong@latrobe.edu.au
[b] Q. Hong, Z. L. Pow, T. C. Owyong, Dr. W. W. H. Wong
School of Chemistry, Bio21 Institute, The University of Melbourne, Parkville, VIC 3010 Australia
^ These authors contributed equally to this work.

it also displayed turn-on fluorescence upon tagging unfolded proteins in vitro and enhanced fluorescence in cells under stress.

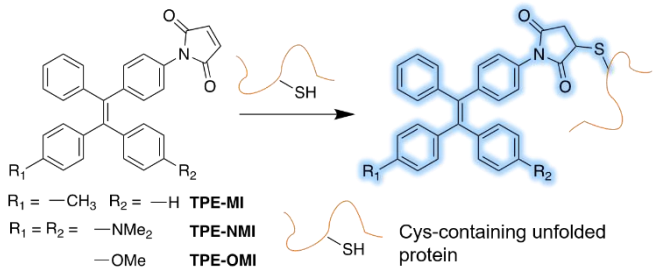


**Figure 1.** Chemical structures of the TPE-MI analogues and the schematic representation of the reaction with a Cys thiol group on unfolded protein to induce fluorescence turn-on effect.

## Results and Discussion

### Dye synthesis and characterization.

Two TPE-MI analogs were designed and synthesized. To improve the water miscibility with minimum structural modification, methoxyl and dimethylamine groups were chosen to functionalize TPE-MI. TPE-NMI and TPE-OMI were synthesized according to the synthetic routes shown in **Scheme 1** in the Experimental Section. All the intermediates and final compounds were fully characterized, and the data were shown in **Figure S1-S7**. Briefly, the precursor N-TPE and O-TPE (**1a** and **1b**) were synthesized via McMurry cross coupling from the two relevant benzophenone derivatives, adopting the previously reported strategies in synthesizing TPE-MI.[5a] The maleimide-containing final product (**2a** and **2b**) was then synthesized by treating with maleic anhydride and sodium acetate in acetic anhydride under reflux condition. Unlike the parent compound TPE-MI,[5b] TPE-NMI and -OMI do not have the *cis*- and *trans*-stereoisomers owing to the symmetrical structure of the benzophenone building blocks.

Following the successful synthesis of TPE-NMI and TPE-OMI, their spectral profiles were measured. Molar absorptivity of both final products was characterized, which is 18,171 and 10,540 $M^{-1}$ $cm^{-1}$ for TPE-NMI and TPE-OMI, respectively, at 350 nm. The normalized absorption spectra show that TPE-OMI exhibits similar absorption maximum as TPE-MI while TPE-NMI shows significant red shift with absorption maximum at approximately 380 nm (**Figure 2A**).

### Monitoring protein unfolding in vitro.

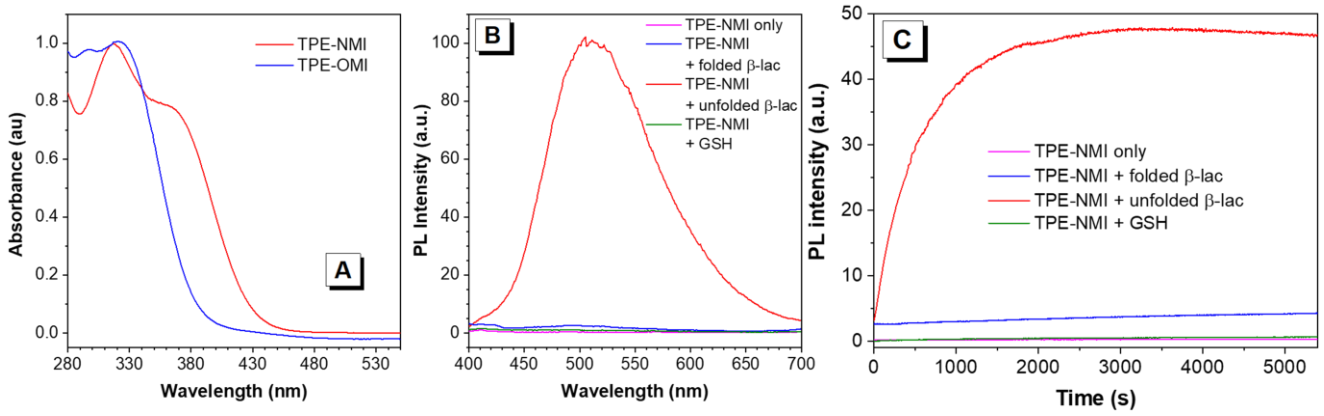


**Figure 2.** (A) Normalized absorption spectra of TPE-NMI and TPE-OMI in DMSO. (B) Emission spectra and (C) fluorescence kinetic plots of TPE-NMI in the presence of folded or unfolded β-lactoglobulin or GSH. Dye concentration = 50 μM. Protein concentration = 50 μM. GSH concentration = 8 mM. Excitation wavelength: 360 nm. Emission wavelength for kinetics: 505 nm.

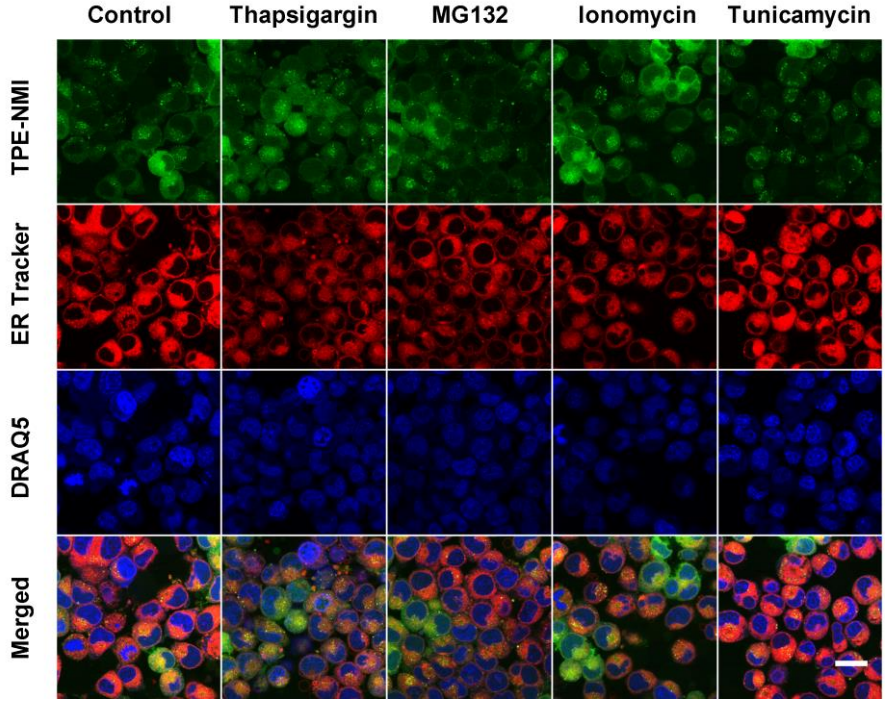


**Figure 3.** Confocal images of untreated and stressed Neuro-2a cells stained with TPE-NMI (50 μM) for 30 min. Four rows show the fluorescence signals in the channel of TPE-NMI (excited at 405 nm, green), ER-Tracker™ Red (excited at 561 nm, red), DRAQ5™ (excited at 640 nm, blue) and merged images, respectively. Scale bar = 20 μm.

The MI moiety can serve as an electron acceptor for the excited donor (TPE moiety), which leads to the quenching of the TPE fluorescence. Therefore, both probes are inherently non-emissive, their emission profiles were thus determined after mixed with unfolded proteins where free Cys thiols were exposed. β-lactoglobulin (β-lac) protein represented an ideal model as it contains two disulfide bonds and a buried free Cys in its folded state.[7] We also tested the reactivity of both dyes with the cytoplasmic thiol-containing tripeptide glutathione (GSH)[8] to evaluate its possible competition for binding to the probes. As illustrated in **Figure 2B** and **S8A**, both TPE-NMI and TPE-OMI exhibited markedly intensified emission in the presence of β-lactoglobulin (50 μM) unfolded by 8 M urea, while the emission maxima were approximately 505 nm and 475 nm, respectively. In sharp contrast, negligible emission was observed in PBS buffer and excess amount of GSH (8 mM), while only a marginal increase in emission was observed in the presence of folded β-lactoglobulin. The subsequent fluorescence kinetic analyses confirmed these results (**Figure 2C** and **S8B**), where both probes displayed progressively enhanced emission over the period of 1.5 hours. These results were in consistency with those observed with TPE-MI,[5b] where the MI moiety exhibited full fluorescence-quenching behavior when not reacting with thiols. The tripeptide GSH failed to induce any emission, indicating that the strong specificity of TPE-MI towards protein thiols was not perturbed by the extra dimethylamine/methoxy substituents in TPE-NMI and -OMI.

**Imaging unfolded proteins in cell.**

As TPE-NMI exhibits more red-shifted spectral profiles compared to the parent compound, TPE-MI, we focused on it for our further biological experiment. Firstly, we evaluated the cytotoxicity of TPE-NMI by AlamarBlue™ cell viability assays. Neuroblastoma 2a (Neuro-2a) cell lines were used in this study. The cells were incubated with this probe at concentrations of 0, 25 or 50 μM for 30 or 60 min. As shown in **Figure S9**, cell viability retained over 90% in all cases, indicating that TPE-NMI incurred insignificant cytotoxicity to the Neuro-2a cells.

To assess the cell permeability of TPE-NMI, we conducted confocal microscopy of the live cells stained with the dye. Upon incubating for 30 min, we observed moderate fluorescence signals mostly located in the cytoplasmic region, indicating that the dye can penetrate cells easily (**Figure 3**). The result also implied that TPE-NMI is excitable with the commonly used 405 nm laser. To check the locations of the dye signals in the cells, the cells were co-stained with ER-Tracker™ Red for ER and DRAQ5™ for nucleus. Signals in three channels were then collected, corresponding to TPE-NMI, ER-Tracker™ Red and DRAQ5™ with excitation wavelength of 405 nm, 561 nm and 640 nm, respectively. To avoid bleed-through and autofluorescence, the settings of three channels were optimized by comparing the fluorescence of single-stained cells in them, shown in **Figure S10**. To verify the cellular localization, we compared the signal from DRAQ5™ and ER-Tracker™ Red with that of TPE-NMI. As illustrated in **Figure 3**, the TPE-NMI fluorescence did not overlap with that of DRAQ5™, indicating that it exhibited good permeability through cell membrane, but

not nuclear membrane. The z-stack slice view in **Figure 4a** and the movie in the supplementary information **Video 1**, further confirmed that the TPE-NMI fluorescence was indeed generated from the intracellular regions. However, the patterns of co-staining with ER-Tracker™ Red were inconclusive. One of the reasons is that TPE-NMI was not evenly distributed in all cells. Despite of a few cells which showed strong TPE-NMI fluorescence, which could be dead cells, the majority of the cells only had very weak TPE-NMI signals. We speculated that the fluorescence signals in the control cells were attributed to the reaction with intrinsically unfolded proteins and newly synthesized proteins that do not fold properly.

intracellular region (**Figure 4b** and **Video 2**). As the aggregation of the dye itself could not produce fluorescence due to the quenching of the maleimide, this observation indicated the potential of using TPE-NMI to visualize aggregation of unfolded proteins in the cells.

The data above showed the potential of TPE-NMI to monitor cellular proteome unfoldedness based on the luminescence change. However, certain limitations cannot be overlooked. For example, confocal microscopy could only analyze cells in a small visual field, which did not reflect the general behavior of this probe and was susceptible to artifacts from dead cells, where fluorescence enhancement might result from the greater

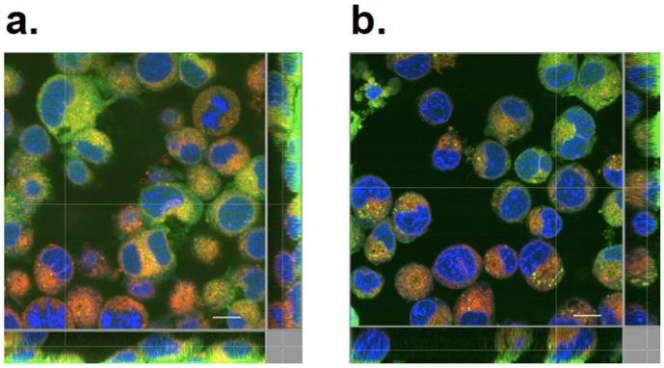


**Figure 4.** Comparison of z-stack slice images show that TPE-NMI could penetrate cell membrane but not nuclear membrane in both control (a) and tunicamycin-treated (b) Neuro-2a cells. TPE-NMI, ER-Tracker™ Red, and DRAQ5™ signals are shown in green, red and blue, respectively. Scale bar = 5

To further induce more unfolded proteins, we treated the cells with different stressors that interfere with the quality control network of the proteins. Four external stress inducers were chosen to perturb different pathways during proteostasis. Tunicamycin is a glycosylation inhibitor that leads to ER accumulation of unfolded proteins that cannot proceed with the calnexin cycle.[9] Thapsigargin is an inhibitor of the calcium ion transportation from cytoplasm to ER and disrupts the function of calcium-dependent ER chaperones, leading to the accumulation of unfolded proteins in the ER.[10] MG132 has been commonly used as an inhibitor of proteolytic activity of the 26S proteasome complex to reduce degradation of ubiquitin-conjugated proteins.[11] Ionomycin can also interfere with the intracellular calcium level and suppress the activity of the mammalian target of rapamycin (mTOR) to disrupt proteostasis in the autophagy pathway.[12] We stained stressed cells with different concentrations of TPE-NMI and compared them with control. As shown in **Figure S11**, TPE-NMI signal was normalized by contrast enhancement with 0.5% saturated pixels, and then visualized by "Fire" lookup table (LUT) color scheme in ImageJ. In some areas, cells treated with MG132 and tunicamycin appeared to display enhancement in luminescence. We also found that cells with elevated level of unfolded proteins exhibited high TPE-NMI fluorescence but somehow lower ER-Tracker™ Red fluorescence. As ER-Tracker™ Red binds to the sulphonylurea receptors of ATP-sensitive $K^+$ channels which are prominent on ER by the moiety of glibenclamide,[13] TPE-NMI might compete for the same binding site. In the z-stack of stressed cells, we could see more brighter aggregates from the amount of luminogens up-taken by cells with compromised cell membrane. To address these issues and further investigate the effectiveness of TPE-NMI in monitoring unfolded protein load in live cells, we performed flow cytometry, which is a commonly used tool for high-throughput and quantitative analyses. Simultaneous detection of multichannel fluorescence in a large cell population by different lasers can be achieved within minutes. We thus aimed to collect the TPE-NMI signal in live cells, which served as an indicator for proteostasis imbalance. The simplified workflow was organized as follow. First, unfolded proteins were induced in cells by different stressors in the same way as conducting cell imaging. Second, cells were stained by TPE-NMI and then TO-PRO-3, a cell-impermeant nucleic acid stain to differentiate live/dead cells.[14] Finally, TPE-NMI signal from live single cells was collected and analyzed by flow cytometry, and the gating strategies are shown in **Figure S12**. Here, utilizing TO-PRO-3 has further confirmed the mechanism how TPE-NMI reports proteostasis imbalances. TO-PRO-3 positive cells were excluded from subsequent analyses. Meanwhile, the percentage of TO-PRO-3 positive cells in the whole population could suggest the condition of stressed cells. TO-PRO-3 negative cells had the same concentrations of TPE-NMI inside cells, because the permeability of TO-PRO-3 was the same among those population of cells. This guaranteed that the difference from TPE-NMI signal resulted from different unfolded protein load in cells, not from different cell permeability.

We incubated cells with tunicamycin and stained them with TPE-NMI, then compared the fluorescence relative to that of control.

The staining protocol was optimized in the preliminary tests, including the TPE-NMI concentration and staining periods, to achieve maximum fluorescence change upon stress (**Figure S13**). We observed that tunicamycin-treated cells stained with 25 μM TPE-NMI for 30 min displayed a significant enhancement in fluorescence in comparison with control and this staining method was used in subsequent experiments. Subsequently, cells were treated with other stressors and stained by the same protocol. The autofluorescence from control and stressed cells may contribute to our readout (**Figure S14**). To address this issue, fluorescence intensity was normalized by subtracting the median signal of TPE-NMI stained cells from the average of the median signal of unstained cells. Our results showed that under all stress conditions that disrupt with proteostasis imbalance, TPE-NMI fluorescence was enhanced significantly (**Figure 5**). This is in accord with an anticipated backlog of cellular unfolded proteins and supports our hypothesis that TPE-NMI can report on the elevated level of unfolded proteins in cells under ER stress that causes accumulation of unfolded proteins.

## Conclusions

Here we described the use of a new fluorescent probe TPE-NMI to assess cellular proteostasis imbalance by targeting the free thiols exposed on the surface of unfolded proteins. We validated this method with model proteins in vitro, and further showed that this probe displayed enhanced fluorescence in cells treated by stressors that induce the backlog of unfolded proteins. In addition, TPE-NMI is a good candidate molecule as the starting point for further optimizations to achieve probes with even more red-shifted photophysical properties, as well as specificity towards the cellular component(s) of interest.

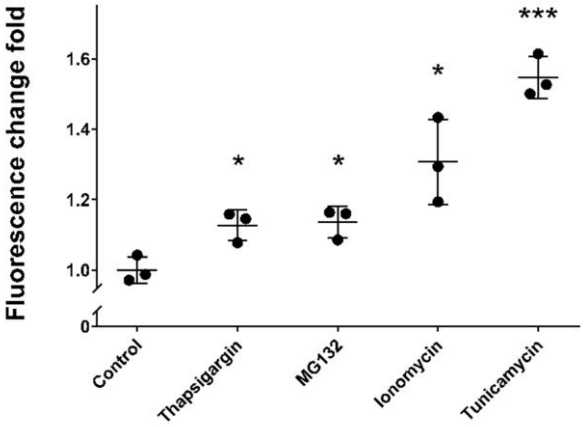


**Figure 5.** TPE-NMI fluorescence increased significantly in cells treated with different stressors (n = 3 biological replicates; mean ± s.e.m.; *, P < 0.05; ***, P < 0.001). Fluorescence intensity was normalized by subtracting median signal of TPE-NMI stained cells from average of median signal of unstained cells. The fluorescence change fold was calculated by the ratio of fluorescence to average of control fluorescence. Raw data were provided in **Table S1**.

## Experimental Section

### Chemical synthesis

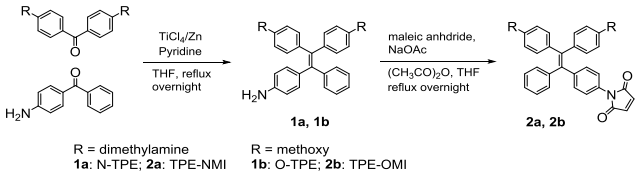


**Scheme S1.** Synthetic routes towards TPE-NMI and TPE-OMI.

**N-TPE (1a).** To a dry 100 ml two-neck RBF were added Zn powder (1.70 g, 26.02 mmol), pyridine (0.30 ml, 3.72 mmol) and anhydrous THF (30.0 ml). The system was fitted with a reflux condenser and purged with $N_2$ three times. After cooling the mixture to 0°C, $TiCl_4$ (1.50 ml, 13.68 mmol) was slowly injected and the mixture was heated under reflux for 30 min. A solution of 4,4'-bis(dimethylamino)benzophenone (886.7 mg, 3.30 mmol) and 4-aminobenzophenone (651.4 mg, 3.30 mmol) in anhydrous THF (20.0 ml) was injected and the mixture was heated under reflux at 90°C overnight. The reaction was quenched by slowly adding saturated $K_2CO_3$ solution and the mixture was filtered. The filtrate was concentrated *in vacuo* then purified by column chromatography (10% EtOAc in PET) to obtain the product (295 mg, isolated yield = 20%). $^1$H NMR (400 MHz, $CDCl_3$): δ (TMS, ppm) 2.87-2.89 (two singlets, 12H), 3.52 (s, 2H), 6.42-6.49 (m, 6H), 6.81-6.94 (m, 6H), 7.02-7.09 (m, 5H). $^{13}$C NMR (100 MHz, $CDCl_3$): δ (TMS, ppm) 40.41, 40.43, 76.68, 77.00, 77.31, 111.35, 111.42, 114.46, 125.30, 127.40, 131.59, 132.41, 132.48, 132.80, 132.96, 135.72, 136.90, 139.60, 143.87, 145.59, 148.54.

**TPE-NMI (2a).** To a stirred solution of N-TPE (100.6 mg, 0.23 mmol) in THF (20.0 ml) were added NaOAc (100.7 mg, 1.40 mmol), acetic anhydride (10.0 ml, 106.0 mmol) and maleic anhydride (47.4 mg, 0.48 mmol). The mixture was heated under reflux overnight. $K_2CO_3$ solution was added and the aqueous phase was extracted three times with DCM. The combined organic phase was washed by brine, dried over anhydrous $Na_2SO_4$ and concentrated *in vacuo*. The product TPE-NMI was recrystallised from isopropanol as an orange power (70.7 mg, isolated yield = 63%). $^1$H NMR (400 MHz, $CDCl_3$): δ (TMS, ppm) 2.89-2.90 (two singlets, 12H), 6.44-6.48 (m, 4H), 6.80 (s, 2H), 6.88-6.93 (m, 4H), 7.05-7.16 (m, 9H). $^{13}$C NMR (100 MHz, $CDCl_3$): δ (TMS, ppm) 55.06, 76.66, 76.93, 76.98, 77.25, 77.30, 112.96, 113.16, 124.88, 126.60, 127.74, 128.98, 131.40, 132.57, 134.12, 135.91, 136.10, 138.12, 140.90, 143.80, 143.89, 158.11, 158.24, 169.45. Molar Absorptivity = 18171 $M^{-1}cm^{-1}$. HRMS (MALDI-TOF) m/z calculated for $C_{34}H_{31}N_3O_2$ 514.24498, found 514.24749.

**O-TPE (1b)**. To a dry 100 ml two-neck RBF were added Zn powder (1.7 g, 26.02 mmol), pyridine (0.4 ml, 4.96 mmol) and anhydrous THF (30.0 ml). The system was fitted with a reflux condenser and purged with $N_2$ three times. After cooling the mixture to 0°C, $TiCl_4$ (2.0 ml, 18.24 mmol) was slowly injected and the mixture was heated under reflux for 30 min. A solution of 4,4'-dimethoxybenzophenone (801.2 mg, 4.06 mmol) and 4-aminobenzophenone (652.2 mg, 3.30 mmol) in anhydrous THF (20.0 ml) was injected and the mixture was heated under reflux at 90°C overnight. The reaction was quenched by slowly adding saturated $K_2CO_3$ solution and the mixture was filtered. The

filtrate was concentrated *in vacuo* then purified by column chromatography to obtain the product (229 mg, isolated yield = 17%). $^{1}$H NMR (400 MHz, $CDCl_3$): δ (TMS, ppm) 3.72-3.75 (two singlets, 6H), 6.41-6.43 (d, 2H), 6.59-6.66 (m, 4H), 6.78-6.80 (d, 2H), 6.89-6.97 (m, 4H), 7.02-7.11 (m, 5H). $^{13}$C NMR (100 MHz, $CDCl_3$): δ (TMS, ppm) 55.05, 76.68, 77.00, 77.32, 112.88, 112.97, 114.39, 125.86, 127.51, 131.45, 132.42, 132.50, 132.55, 134.61, 136.79, 136.94, 138.44, 139.21, 144.40, 144.66, 157.76.

**TPE-OMI (2b).** To a stirred solution of O-TPE (101.6 mg, 0.25 mmol) in THF (20.0 ml) were added NaOAc (105.0 mg, 1.45 mmol), acetic anhydride (10.0 ml, 105.98 mmol) and maleic anhydride (48.8 mg, 0.50 mmol). The mixture was heated under reflux overnight. $K_2CO_3$ solution was added and the aqueous phase was extracted three times with DCM. The combined organic phase was washed by brine, dried over anhydrous $Na_2SO_4$ and concentrated *in vacuo*. The product TPE-OMI was purified by column chromatography and recrystallised from petroleum ether as a yellow powder (11.2 mg, isolated yield = 9%). $^{1}$H NMR (400 MHz, $CDCl_3$): δ (TMS, ppm) 3.74-3.75 (two singlets, 6H), 6.62-6.67 (m, 4H), 6.81 (s, 2H), 6.92-6.97 (m, 4H), 7.02-7.04 (m, 2H), 7.09-7.12 (m, 7H). $^{13}$C NMR (100 MHz, $CDCl_3$): δ (TMS, ppm) 20.56, 20.59, 125.82, 126.01, 126.97, 127.07, 127.13, 127.16, 127.75, 127.95, 128.61, 130.55, 130.67, 130.70, 130.74, 130.78, 131.27, 131.31, 133.53, 135.59, 135.77, 138.74, 139.68, 139.90, 141.07, 142.76, 142.92, 143.13, 168.83. Molar Absorptivity = 10540 $M^{-1}cm^{-1}$. HRMS (MALDI-TOF) m/z calculated for $C_{32}H_{25}NO_4$ 488.18171, found 488.18562.

**Mammalian cell culturing**

Neuro-2a cell lines (from lab cultures originally obtained from ATCC) were maintained in Dulbecco's modified Eagles Medium (DMEM) supplemented with 10% v/v fetal bovine serum at 37°C in a humidified incubator with 5% atmospheric $CO_2$. For cell viability assay, $3\times10^4$ Neuro-2a cells were plated on 96-well plates. For flow cytometry, $4\times10^5$ Neuro-2a cells were plated on 12-well plates. For microscopy experiments, $8\times10^4$ Neuro-2a cells were plated on 8-well μ-slides (Ibidi).

**Cell viability assay**

Seeded Neuro-2a cells were cultured overnight to reach approximately 80% confluency. Then the cells were rinsed with PBS and stained with 25 μM or 50 μM of freshly diluted TPE-NMI in PBS at 37 °C for 30 or 60 min. Cells were also treated with corresponding amount of DMSO to exclude the cytotoxicity of DMSO. Afterwards cells were rinsed with PBS again and incubated with 10% alamarBlue™ reagent in complete DMEM at 37°C for 4 hours in darkness. The alamarBlue™ reagent was excited at the wavelength of 540–570 nm, and emission was recorded at 580–610 nm by plate reader. Positive controls (by killing cells with 70% ethanol) and negative controls (cultured in complete DMEM without any treatment) were properly set. Cytotoxicity was calculated by the following formula: Normalized cell viability = (sample RFU - positive control RFU) / (negative control RFU - positive control RFU), where RFU represents "relative fluorescence units".

**Confocal microscopy imaging**

Seeded Neuro-2a cells were cultured overnight to reach approximately 80% confluency, and then treated with different stressors as described above. Then cells were rinsed with PBS and stained with 25 μM or 50 μM of freshly diluted TPE-NMI in PBS at 37°C for 30 min. Subsequently, cells were rinsed with PBS and stained with freshly diluted 5 μM of DRAQ5™ and 1 μM of ER-Tracker™ Red in DMEM at 37°C for 20 min. After staining, cells were rinsed with PBS again, fixed with 4% (w/v) paraformaldehyde at 37°C for 5 min, rinsed with PBS, and maintained in PBS for microscopy. Cells were imaged on a Zeiss LSM800 confocal microscope for TPE-NMI (excitation: 405 nm, emission: 450–520 nm), ER-Tracker Red (excitation: 561 nm, emission: 560–620 nm) and DRAQ5 (excitation: 640 nm, emission: 650–700 nm) using a 63× objective lens.

**Flow cytometry**

Seeded Neuro-2a cells were cultured overnight to reach approximately 80% confluency, and then treated with novobiocin (800 μM), thapsigargin (12 μM), MG132 (20 μM) or ionomycin (10 μM) for 4 hours, or with tunicamycin (5 μg/ml) for 18 hours. Stressed cells were rinsed with PBS and stained with 25 μM of freshly diluted TPE-NMI in PBS at 37°C for 30 min. After staining, cells were rinsed with PBS again and resuspended in 0.4 μM TO-PRO-3 diluted in PBS for flow cytometric assay in three biological replicates. Cells were analyzed at a high flow rate in a BD FACS Canto II instrument and 30,000–50,000 events were collected. Data were collected from the APC channel ($\lambda_{ex}$: 635 nm, $\lambda_{em}$: 660 ± 20 nm) and the V500 channel ($\lambda_{ex}$: 405 nm, $\lambda_{em}$: 525 ± 20 nm) for detecting TO-PRO-3 and TPE-NMI signal, respectively. The gating strategies are shown in **Figure S9**. Fluorescence intensity was normalized by subtracting the median signal of TPE-NMI stained cells from the average of the median signal of unstained cells. The fluorescence change fold was calculated by the ratio of fluorescence to average of control fluorescence. Flow cytometry data were analyzed with FlowJo (Tree Star Inc.). Graphs were analyzed, and statistical analyses were performed using Prism (GraphPad) software packages. Raw data were provided in **Table S1**.

## Acknowledgements

We thank Dr Peter Lock and LIMS BioImaging Platform, La Trobe University for the technical support and access to the confocal microscope and flow cytometer. We also thank A/Prof Danny Hatters from The University of Melbourne for helpful discussion. This work was supported by grants to Y.H.

(Australian Research Council DE170100058 and Rebecca L. Cooper Medical Research Foundation PG2018043).

**Keywords:** Aggregation-induced emission • tetraphenylethene • fluorescent probe • cell imaging

## References

[1] a) R. Inagi, Y. Ishimoto, M. Nangaku, *Nat. Rev. Nephrol.* **2014**, *10*, 369-378; b) M. Radwan, R. J. Wood, X. Sui, D. M. Hatters, *IUBMB Life.* **2017**, *69*, 49-54; c) W. Scheper, J. J. M. Hoozemans, *Acta Neuropathol.* **2015**, *130*, 315-331.

[2] a) G. M. Ashraf, N. H. Greig, T. A. Khan, I. Hassan, S. Tabrez, S. Shakil, I. A. Sheikh, S. K. Zaidi, M. A. Wali, N. R. Jabir, C. K. Firoz, A. Naeem, I. M. Alhazza, G. A. Damanhouri, M. A. Kamal, *CNS Neurol. Disord. Drug Targets* **2014**, *13*, 1280-1293; b) J. Kirstein, D. Morito, T. Kakihana, M. Sugihara, A. Minnen, M. S. Hipp, C. Nussbaum‐Krammer, P. Kasturi, F. U. Hartl, K. Nagata, R. I. Morimoto, *EMBO J.* **2015**, *34*, 2334-2349; c) C. A. Ross, M. A. Poirier, *Nat. Med.* **2004**, *10*, S10-S17.

[3] M. Wang, R. J. Kaufman, *Nature* **2016**, *529*, 326-335.

[4] a) R. Gupta, P. Kasturi, A. Bracher, C. Loew, M. Zheng, A. Villella, D. Garza, F. U. Hartl, S. Raychaudhuri, *Nat. Methods* **2011**, *8*, 879-884; b) Y. Liu, X. Zhang, W. Chen, Y. L. Tan, J. W. Kelly, *J. AM. Chem. Soc.* **2015**, *137*, 11303-11311; c) Y. Liu, M. Fares, N. P. Dunham, Z. Gao, K. Miao, X. Jiang, S. S. Bollinger, A. K. Boal, X. Zhang, *Angew. Chem. Int. Ed. Engl.* **2017**, *56*, 8672-8676; d) Y. Liu, C. H. Wolstenholme, G. C. Carter, H. Liu, H. Hu, L. S. Grainger, K. Miao, M. Fares, C. A. Hoelzel, H. P. Yennawar, G. Ning, M. Du, L. Bai, X. Li, X. Zhang, *J. AM. Chem. Soc.* **2018**, *140*, 7381-7384; e) Y. Liu, Y. L. Tan, X. Zhang, G. Bhabha, D. C. Ekiert, J. C. Genereux, Y. Cho, Y. Kipnis, S. Bjelic, D. Baker, J. W. Kelly, *Proc. Natl. Acad. Sci. U.S.A.* **2014**, *111*, 4449-4454; f) R. J. Wood, A. R. Ormsby, M. Radwan, D. Cox, A. Sharma, T. Vöpel, S. Ebbinghaus, M. Oliveberg, G. E. Reid, A. Dickson, D. M. Hatters, *Nat. Commun.* **2018**, *9*, 287.

[5] a) Y. Liu, Y. Yu, J. W. Y. Lam, Y. Hong, M. Faisal, W. Z. Yuan, B. Z. Tang, *Eur. J. Chem.* **2010**, *16*, 8433-8438; b) M. Z. Chen, N. S. Moily, J. L. Bridgford, R. J. Wood, M. Radwan, T. A. Smith, Z. Song, B. Z. Tang, L. Tilley, X. Xu, G. E. Reid, M. A. Pouladi, Y. Hong, D. M. Hatters, *Nat. Commun.* **2017**, *8*, 474-484.

[6] S. M. Marino, V. N. Gladyshev, *J. Mol. Biol.* **2010**, *404*, 902-916.

[7] a) R. Bauer, S. Hansen, L. Ødgendal, *Int. Dairy J.* **1998**, *8*, 105-112; b) E. M. Dumay, M. T. Kalichevsky, J. C. Cheftel, *Food Sci. Technol.* **1998**, *31*, 10-19; c) D. Renard, J. Lefebvre, P. Robert, G. Llamas, E. Dufour, *Int. J. Biol. Macromol.* **1999**, *26*, 35-44.

[8] R. E. Hansen, D. Roth, J. R. Winther, *Proc. Natl. Acad. Sci. U.S.A.* **2009**, *106*, 422-427.

[9] S.-W. Chan, P. A. Egan, *The FASEB Journal* **2005**, *19*, 1510-1512.

[10] a) C. M. Oslowski, F. Urano, in *Methods in Enzymology, Vol. 490* (Ed.: P. M. Conn), Academic Press, **2011**, pp. 71-92; b) I. G. Ganley, P.-M. Wong, N. Gammoh, X. Jiang, *Mol. Cell* **2011**, *42*, 731-743.

[11] L. Zhang, H. Tang, Y. Kou, R. Li, Y. Zheng, Q. Wang, X. Zhou, L. Jin, *Journal of Cancer Research and Clinical Oncology* **2013**, *139*, 1105-1115.

[12] R. Sano, J. C. Reed, *Biochimica et Biophysica Acta (BBA) - Molecular Cell Research* **2013**, *1833*, 3460-3470.

[13] X. Serrano-Martín, G. Payares, A. Mendoza-León, *Antimicrobial agents and chemotherapy* **2006**, *50*, 4214-4216.

[14] L. Jiang, R. Tixeira, S. Caruso, G. K. Atkin-Smith, A. A. Baxter, S. Paone, M. D. Hulett, I. K. Poon, *Nat Protoc* **2016**, *11*, 655-663.

# FULL PAPER

**Stress proteins out**. TPE-NMI probes unfolded proteins by targeting cysteines located in a hydrophobic environment. Upon thiol conjugation via maleimide and restriction of intramolecular rotation, its fluorescence quantum yield increases dramatically. Based on this mechanism, we have shown TPE-NMI can turn on fluorescence upon reacting with unfolded proteins in vitro and in live cells under proteostatic stress conditions.